ORIGINAL PAPER

Scanning electrochemical microscopy study of ion transfer process across water/2-nitrophenyloctylether interface supported by hydrophobic carbon ceramic electrode

Galyna Shul · Wojciech Nogala · Iryna Zakorchemna · Joanna Niedziolka · Marcin Opallo

Abstract A carbon ceramic electrode (CCE) modified with the redox probe—decamethylferrocene solution in hydrophobic organic solvent—2-nitrophenyloctyl ether and immersed into an aqueous solution was studied by scanning electrochemical microscopy (SECM). After the electrochemical oxidation of decamethylferrocene, its cations were detected near the electrode surface in the aqueous phase. This indicates that some fraction of the redox-active cations electrochemically produced in the organic phase is transferred across the liquid/liquid interface. They are reduced at the SECM tip and form a solid deposit. The amount of deposited decamethylferrocene was estimated by the anodic reaction at the tip. It is affected by the substrate–tip distance, deposition time, and electrolyte concentration. The SECM images of unmodified and modified CCEs are consistent with their heterogeneous structure.

Keywords Carbon ceramic electrode ·
Scanning electrochemical microscopy (SECM) ·
Decamethylferrocene · Ion transfer · Liquid/liquid interface

Introduction

The electrochemical processes occurring at the interface between two immiscible liquids are interesting from both fundamental and practical point of views [1]. The ion transfer across the liquid/liquid interface is one of the most important phenomena in biological systems and in chemical technology like separation, extraction, or organic synthesis, etc. [1]. In recent years, several groups designed and studied novel systems—so-called three-phase electrodes [2, 3]. Typically, they are based on a small volume of hydrophobic liquid deposited on the electrode surface immersed into the aqueous solution where the electrogenerated ion transfer between two immiscible liquids is observed [2–7]. In this case, the formation and the transport of charged species across the liquid/liquid interface in the three-phase systems (organic phase/aqueous phase/solid conductor) are strongly coupled to the electrooxidation of the redox probe present in one of the liquid phases. The ion transfer across the liquid/liquid interface takes place to maintain the electroneutrality in both liquids [2–8]. Among the different electrode materials used for the three-phase electrodes, a hydrophobic silica carbon composite material called carbon ceramic electrode (CCE) [9, 10] was proposed [11, 12]. The combination of a porous matrix with graphite microparticles forming percolation paths provides a suitable environment for the formation of an extended three-phase junction, organic phase/aqueous electrolyte/graphite particle, thereby enhancing the efficiency of the electrode process [13–15].

Decamethylferrocene (DMFc) was widely used as hydrophobic redox probe to generate liquid/liquid ion transfer at the three-phase electrodes [3, 5, 7, 8, 16–18]. On the basis of a simple thermodynamic analysis of its redox potential shift, it has been shown that electrooxidation of this probe in the organic phase,

$$\text{DMFc}_{(org)} - \text{e}^-_{(electrode)} \leftrightarrow \text{DMFc}^+_{(org)} \tag{1}$$

is followed solely by an anion X^- insertion into the organic phase [3, 5, 7, 8, 16–18],

$$\text{DMFc}^+_{(org)} + X^-_{(aq)} \rightarrow \text{DMFc}^+_{(org)} + X^-_{(org)}. \tag{2}$$
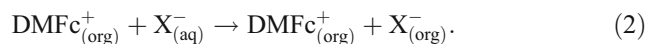
G. Shul · W. Nogala · I. Zakorchemna · J. Niedziolka ·
M. Opallo (✉)
Institute of Physical Chemistry, Polish Academy of Sciences,
Kasprzaka 44/52,
01-224 Warsaw, Poland
e-mail: mopallo@ichf.edu.pl

Hence, the ion transfer in the opposite direction—the ejection of the electrogenerated DMFc$^+$ into the aqueous solution—has not been taken into account, except for strongly hydrophilic anions like F$^-$ or SO$_4^{2-}$ [5, 13]. It is interesting to note that the leaching of absorbed dimethylferrocene from amperometric enzyme electrodes into the aqueous phase was earlier recognized by Schuhmann et al. [19].

In this report, we show that a part of the electrochemically generated DMFc$^+$ ions in the hydrophobic organic phase supported by CCE are ejected into the aqueous electrolyte solution. This was possible with the use of scanning electrochemical microscopy (SECM) [20–23]. This technique allows for the detection of electroactive ions close to the electrode surface and in a specifically set place. Earlier, the ion transfer across the polarized liquid/liquid interface was investigated by SECM with a micropipette tip [24, 25]. Also, the three-phase reaction occurring at a DMFc solution in nitrobenzene/aqueous solution/glassy carbon electrode was studied with an ultramicroelectrode positioned at three different parts of the nitrobenzene droplet deposited at the electrode surface [26]. In this report, for the first time, conventional SECM is employed to study the unmodified CCE and the CCE modified with DMFc solution in o-nitrophenyloctyl ether (NPOE). For the latter electrode, the mechanism of the electrochemical reaction described by Eqs. 1 and 2 was already proven on the basis of thermodynamic analysis [5, 13].

Experimental

Chemicals

DMFc (97%), 1,1′-ferrocenedimethanol (Fc(CH$_2$OH)$_2$) (98%), used as redox probes, and methyltrimethoxysilane (MTMOS) (99%) were obtained from Aldrich; the organic solvent NPOE (99+%) was obtained from Fluka. KCl and NaClO$_4$ (analytical grade) were purchased from POCh. Graphite powder MP-300 with average particle size 20 μm was from Carbon GmbH. All aqueous solutions were prepared from deionized water (ELIX system, Millipore).

Substrate preparation and modification

The CCE was prepared as described elsewhere [9, 10]. The hydrolyzed sol obtained by mixing 1 ml of MTMOS with 1.5 ml of methanol was sonicated for 2 min after the addition of 50 μl of 11 M HCl. Next, 1.25 g of graphite powder was added and the mixture was sonicated for another minute. The resulting mixture was placed into a 2-mm deep cavity of glass tubing, 1.55 mm inner diameter filled tightly with a copper wire. The electrode was left for drying for at

least 48 h at room temperature and then it was polished with emery paper. The geometric surface area was 0.019 cm^2. The CCE was modified with 2 μl of 0.01 mol dm^{-3} DMFc solution in NPOE that was sprinkled on the top of the electrode. After impregnation, the remains of the modifier were gently dried off with tissue paper. For each experiment, a freshly modified electrode was employed.

Apparatus and procedures

All electrochemical experiments were carried out with SECM (CHI900B) in a Faraday cage. A four-electrode arrangement was used with CCE, and a Pt ultramicroelectrode as working electrodes, and Ag/AgCl/KCl(sat.) and a Pt wire as reference and counter electrodes, respectively. The stage with the SECM substrate (CCE) was fixed at the bottom of the cell. The SECM tip (10 μm diameter Pt disk ultramicroelectrode) was driven by computer-controlled stepper motors allowing movements in the x, y, and z directions with a resolution of 100 nm. All experiments (unless otherwise stated) were performed in aqueous KCl solutions of different concentrations. They were carried out at room temperature (21±2°C).

The X-ray photoelectron spectroscopy (XPS) spectra were recorded on a VG Microtech system equipped with an Al anode (hν=1486.6 eV). Concentration–depth profiling was performed by Ar sputtering of 10 μA/cm^2 at 3.0 kV. As a substrate for these experiments, a Pt disk electrode (diameter=1.5 cm) was used.

Results and discussion

Probing DMFc$^+$ transfer across the liquid/liquid interface by SECM tip and XPS analysis

First, a SECM approach curve was obtained. The tip was biased at −0.5 V vs Ag/AgCl—the potential corresponding to the electroreduction of dioxygen. It was moved toward the CCE surface and the current was recorded as a function of the distance (d). The distance $d≈0$ was assumed when the current decreased down to 80% of that recorded in bulk solution. This negative feedback effect is caused by the hindered diffusion of dioxygen [22]. Then, the tip was moved back a few micrometers depending on the task.

The method of detection of DMFc$^+$ transfer across the liquid/liquid interface supported by the CCE is based on the electrochemical reduction of the DMFc$^+$ cations at the SECM tip followed by the electrochemical dissolution of the formed precipitate. Therefore, the SECM tip (Pt ultramicroelectrode) and the SECM substrate (CCE) potentials have to be appropriately related to the redox potential of the DMFc/DMFc$^+$ redox couple (E^0) obtained from cyclic
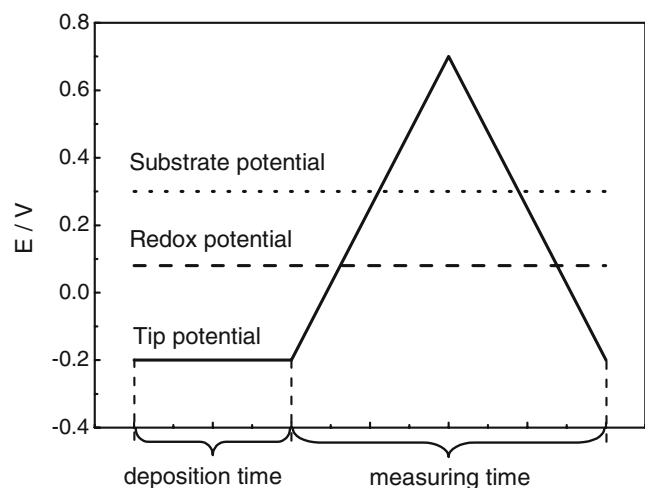
Scheme 1 A schematic presentation of the applied potential program at the SECM tip (*solid line*) and the SECM substrate (*dotted line*). The *dashed line* indicates the redox potential of the $DMFc^+/DMFc$ couple obtained for a CCE modified with DMFc solution in NPOE immersed into 0.1 mol dm^{-3} aqueous KCl solution

voltammetry of the CCE modified with DMFc in NPOE and immersed into the aqueous salt solution [13]. The potential program of both substrate and tip is shown in Scheme 1. The substrate potential was set higher than E^0 to generate $DMFc^+$ cations in the organic phase. On the other hand, the tip potential in the first step, deposition, was set lower than E^0 to allow for the electrodeposition of DMFc from the aqueous solution. In the second step, measurement, cyclic voltammetry with a scan rate equal to 50 mV s^{-1} was performed at the tip.

The first experiments were performed in 0.1 mol dm^{-3} aqueous KCl solution. On the voltammograms obtained on the SECM tip, only an anodic peak is observed (Fig. 1). No
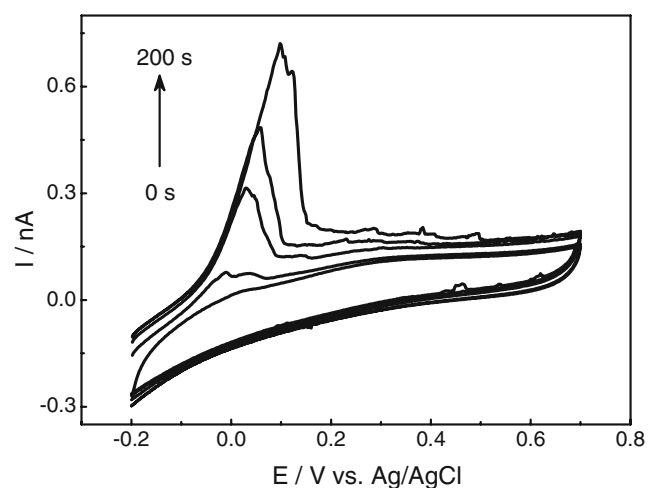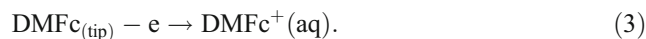
voltammetric signal is obtained in analogous experiments without potential applied to the unmodified CCE substrate or the CCE modified with pure NPOE. Therefore, the observed signal can be tentatively ascribed to the electro-dissolution of DMFc:

$$DMFc_{(tip)} - e \rightarrow DMFc^+(aq). \quad (3)$$

The absence of a cathodic peak indicates the total stripping of the organic deposit.

Because the $DMFc^+$ cations are initially absent in the aqueous solution, one may conclude that the deposition of DMFc on the tip results from the $DMFc^+$ cation transfer across the liquid/liquid interface:

$$DMFc_{(org)}^+ \rightarrow DMFc_{(aq)}^+. \quad (4)$$
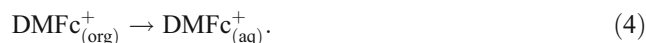
The magnitude of the anodic peak is proportional to the deposition time (t), confirming that the voltammetric signal recorded on the tip is bound to the electrochemical generation of $DMFc^+$ cations in the organic phase (Eq. 1). The decrease of the anodic peak current with an increase of the distance between tip and CCE (Fig. 2) is caused by the $DMFc^+$ concentration gradient in the aqueous solution.

It is reasonable to assume that the number of $DMFc^+$ cations ejected across the liquid/liquid interface is proportional to the amount of the DMFc deposit on the SECM tip. The last quantity can be obtained from the anodic charge passed during DMFc electrodissolution (Q). Not surprisingly, we found the Q value to be proportional to t, and this linear dependence approximately passes the origin (Fig. 3). We made an attempt to estimate the local concentration of $DMFc^+$ next to the substrate by assuming that the diffusion of $DMFc^+$ to the SECM tip is predominantly hemispherical.
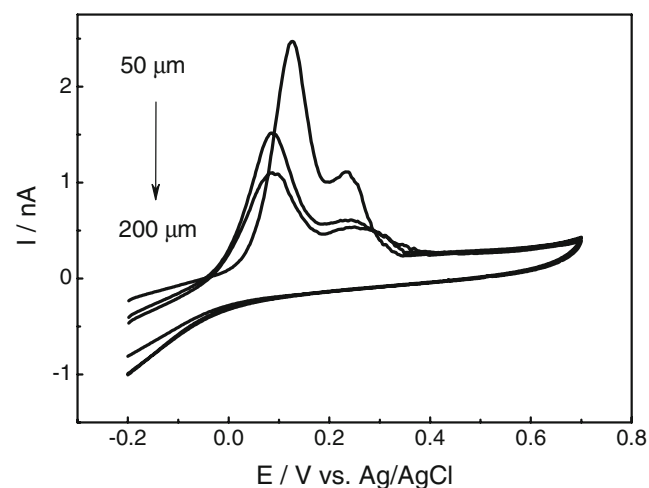

Fig. 1 Cyclic voltammograms obtained at the SECM tip at 100 μm distance from the surface of the CCE modified with 0.01 mol dm^{-3} DMFc solution in NPOE and immersed into 0.01 mol dm^{-3} aqueous KCl solution. The *arrow* shows the increase of the deposition time (0, 10, 50, 100, and 200 s) at a potential of −0.2 V. Scan rate=0.05 V s^{-1}

Fig. 2 Cyclic voltammograms obtained at the SECM tip at 50, 100, and 200 μm distances from the surface of the CCE modified with 0.01 mol dm^{-3} DMFc solution in NPOE and immersed into 0.001 mol dm^{-3} aqueous KCl solution. The voltammograms were obtained after 100 s deposition time at a potential of −0.2 V. Scan rate=0.05 V s^{-1}
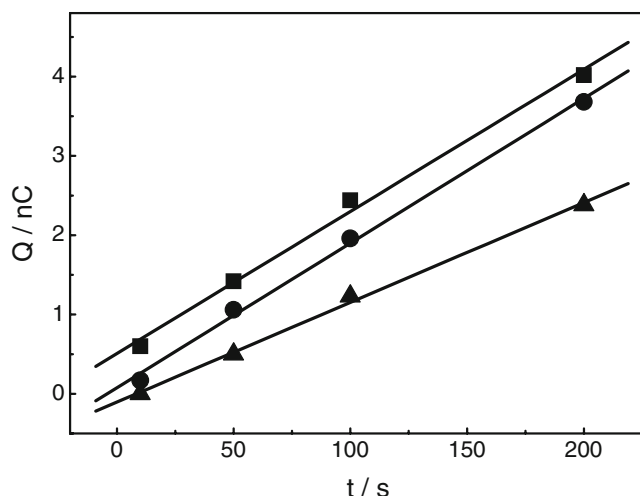
Fig. 3 Plot of anodic charge (Q) vs deposition time (t). The Q values were calculated from cyclic voltammograms obtained with the SECM tip at 50 μm (*closed squares*), 100 μm (*closed circles*), and 200 μm (*closed triangles*) distances from the surface of the CCE modified with 0.01 mol dm^{-3} DMFc solution in NPOE and immersed into 0.01 mol dm^{-3} aqueous KCl solution. The *solid lines* were obtained by linear regression

Therefore, the steady-state current (I) corresponding to DMFc electrodeposition at the disk with radius (r) can be calculated from the anodic charge passed during the DMFc electrodeposition and the deposition time. The diffusion coefficient of DMFc^{+} in water (D) is estimated to 1×10^{-5} cm^2 s^{-1}. The estimate was made on the basis of the value obtained in dichloromethane [27] taking into account the solvent viscosity ratio. This value compares well with the experimentally estimated diffusion coefficient of ferrocene in water [28]. The DMFc^{+} cation concentration (C^0) can be estimated from the following equation:

$$C^0 = \frac{I}{4nFDr} = \frac{Q}{4nFDrt}. \tag{5}$$

From the experiment with the longest electrolysis, the largest value of the DMFc^{+} concentration is estimated. It equals 10^{-5} mol dm^{-3} and compares well with the solubility of less hydrophobic monoalkylferrocenium salts equal to 10^{-4} to 10^{-3} mol dm^{-3} [29, 30]. Obviously, this is a rough estimate because the collection efficiency of the tip is below unity. The result may be also affected by the blocking of the electrode surface by DMFc deposit and its peeling off from the tip. In addition, Eq. 5 is valid for a diffusion-controlled reaction at a disk microelectrode under steady-state conditions. These can be disturbed by the DMFc^{+} concentration gradient if the SECM tip is placed in the expanding diffusion layer of the CCE. Therefore, the time of the experiment has to be limited. The obtained results seem to show that this method enables us to detect and compare small quantities (low concentration in a thin diffusion layer) of DMFc in the aqueous solution. The observed propor-

tionality of Q vs t (see Fig. 8) confirms that this is a good method.

The next experiments were performed at KCl concentrations higher and lower than the DMFc concentration in the organic phase. The smaller concentration of supporting electrolyte, the larger DMFc electrodissolution peak current is observed (Fig. 4), indicating the larger amount of DMFc^{+} transferred across the liquid/liquid interface. This may be explained as a result of a deficiency of Cl^{-} anions next to the interface. If the flux of anions is not big enough to compensate the newly formed DMFc^{+} cations, they are ejected into the aqueous solution and the contribution of reaction 2 decreased.

Another important effect is observed when hydrophilic Cl^{-} anions in the aqueous phase are replaced by more hydrophobic ClO$_4^{-}$. This change causes a decrease of the peak current (Fig. 5), indicating that under these conditions, the number of DMFc^{+} anions ejected into the aqueous phase is decreased. This is connected with the different values of ClO$_4^{-}$ and Cl^{-} anion transfer potential across the NPOE/water interface. They are equal to -0.175 and -0.521 V, respectively [31]. This experiment shows that in the presence of more hydrophobic anions the contribution of reaction 4 is smaller and a larger number of electrogenerated DMFc^{+} cations is compensated in the organic phase than in the case of less hydrophobic anions present in the aqueous phase. Moreover, the reaction zone is not limited to the three-phase junction because of the insertion of counterions into the organic phase [7].

It is interesting to note that an indication of the electrochemical generation of hydrophobic DMFc^{+} can be found in literature. Bond and Marken [32] reported the unstable voltammetry of a graphite electrode with mechanically
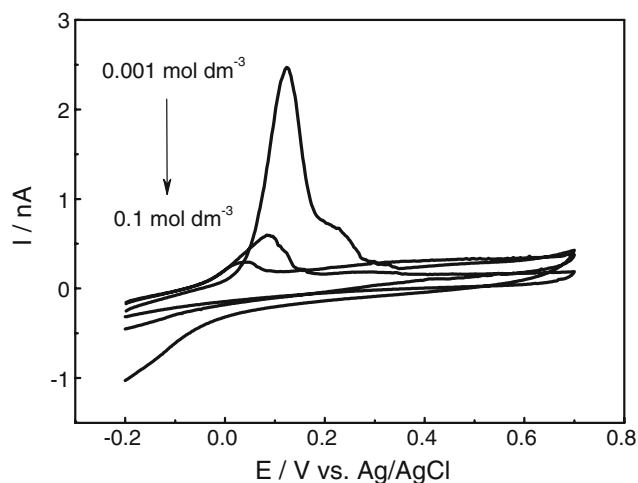

Fig. 4 Cyclic voltammograms obtained at the SECM tip at 50 μm distances from the surface of CCE modified with 0.01 mol dm^{-3} DMFc solution in NPOE and immersed into aqueous 0.001, 0.01, and 0.1 mol dm^{-3} KCl solution. The voltammograms were obtained after 200 s deposition time at a potential of -0.2 V. Scan rate=0.05 V s^{-1}
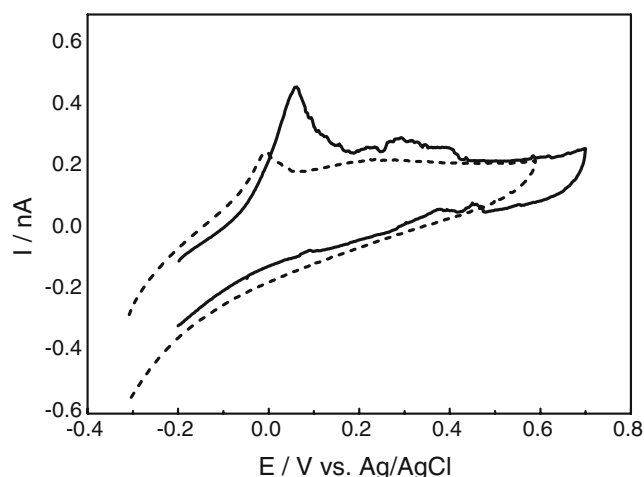
Fig. 5 Comparison of the cyclic voltammograms obtained at the SECM tip at 200 μm distances from the surface of the CCE modified with 0.01 mol dm^{-3} DMFc solution in NPOE and immersed into 0.1 mol dm^{-3} KCl (*solid*) and NaClO$_4$ (*dotted*) aqueous solution. The voltammograms were obtained after 200 s deposition time at a potential of −0.2 V (KCl) and −0.3 V (KClO$_4$). Scan rate=0.05 V s^{-1}

attached solid DMFc particles and immersed in the aqueous electrolyte. The observed decrease of the peak current in subsequent scans is more pronounced for more hydrophilic anions present in the aqueous phase. The authors claimed that this results from a loss of DMFc from the graphite electrode surface into the solution [32].

The presence of iron in the organic deposit on the tip was confirmed by XPS experiments. To prepare the sample, an experiment similar to that described above was performed with a large Pt disk electrode. The Pt disk was fixed about 1–2 mm to the surface of the CCE modified with NPOE or DMFc solution in NPOE. Both electrodes were placed in the four-electrode cell together with counter and reference electrodes. The potentials of −0.2 and 0.3 V were applied to the Pt disk and the CCE electrodes, respectively, during 36 h. After that the Pt disk was removed and rinsed carefully with water.

Figure 6a shows the XPS spectra in the binding energy range 700–740 eV. This energy region was chosen because of the strongest photoelectron peak $2p_{3/2}$ for iron at 710 eV and the adjacent peak for platinum at 726 eV. In the initial spectrum, both peaks for iron and platinum are dimmed because of the adsorbed impurities from the atmosphere (mainly oxygen and carbon, distinctly visible in the full range spectrum, not shown here). However, the expected peak for iron is clearly visible after about 2 min of Ar sputtering. After 10 min of Ar sputtering, the surface layer was completely removed and the spectrum was identical with the Pt substrate. Comparing the height of the strongest peak $2p_{3/2}$ for iron with the strongest peak $4f_{7/2}$ for platinum (observed on the full spectrum), it is evident that the detected iron can be considered as a trace amount. On the other hand, the spectrum of the sample obtained from

the blank electrochemical experiment with unmodified CCE shows the absence of the iron signal (Fig. 6b).

SECM imaging of CCEs

At first, the SECM imaging of the unmodified CCE was performed by exploring the feedback diffusion of the redox probe—Fc(CH$_2$OH)$_2$—dissolved in the aqueous solution in feedback mode. In these experiments, the surface area of 400×400 μm was scanned with the tip positioned at approximately 3 μm distance from the point $d\approx0$.

Clearly, the magnitude of the current connected with the electrooxidation of the redox probe depends on the position of the tip in the x–y plane (Fig. 7). The irregular maxima and minima of the tip current indicate that only parts of the CCE surface are electrochemically active. This picture is consistent with the earlier observation by scanning electron microscopy [13, 33]. This method allowed for the detection of small and irregular aggregates of graphite particles ranging from 20 to almost 100 μm surrounded by silicate matrix [13, 33]. It is interesting to note that the similar features of the SECM images for the unmodified CCE and the CCE modified with NPOE are observed (Fig. 8). This
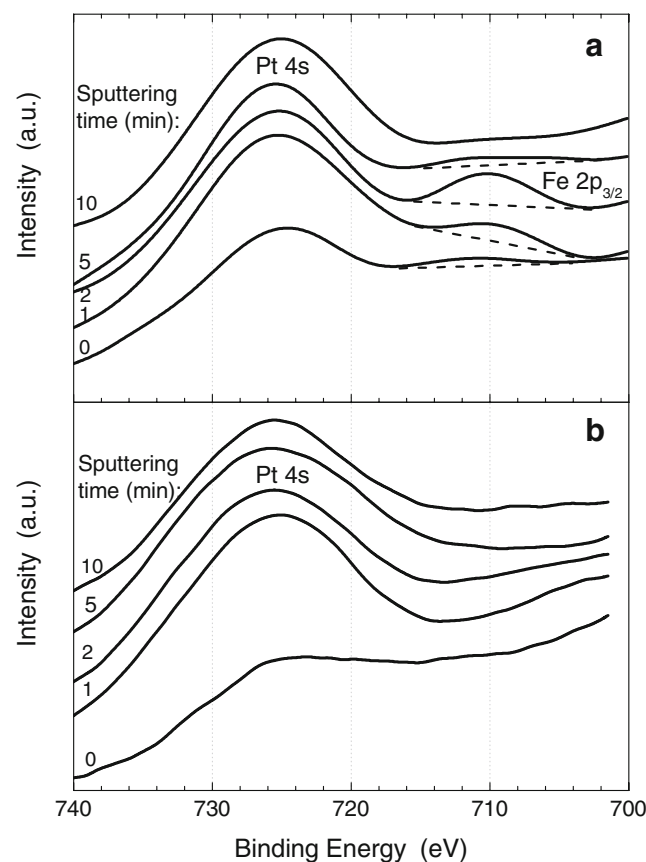

Fig. 6 XPS spectra from the Pt surface working as the electrode in the four-electrode cell (see text) and placed near a CCE modified with DMFc solution in NPOE (**a**) or modified with pure NPOE (**b**) as a function of Ar sputtering
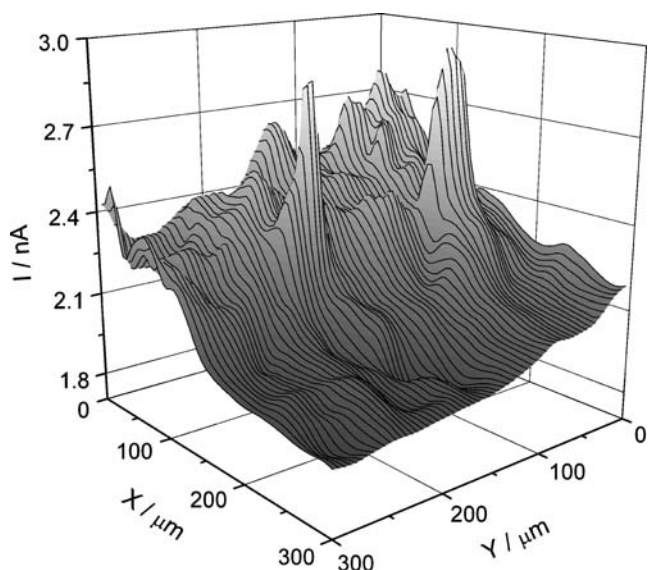
Fig. 7 SECM image of the CCE immersed into 0.001 mol dm^{-3} Fc(CH$_2$OH)$_2$ solution in 0.1 mol dm^{-3} aqueous KCl. The potential of the SECM tip was set at 0.5 V vs Ag/AgCl, no potential was applied to the CCE (feedback mode), $d{\approx}3$ μm

Fig. 9 SECM image of the CCE modified with 0.01 mol dm^{-3} DMFc solution in NPOE and immersed into 0.1 mol dm^{-3} aqueous KCl solution. The potential of the SECM tip and the CCE were set at 0 and 0.5 V vs Ag/AgCl, respectively (SG/TC mode), $d{\approx}3$ μm

indicates that the surface of the graphite particles facing the aqueous electrolyte is not completely covered by the organic solvent. Namely, the three-phase junctions, NPOE/ aqueous phase/graphite, indispensable for reaction 1 are formed.

Next, we made an attempt of imaging of the CCE modified with DMFc solution in NPOE. This was performed in substrate generation/tip collection (SG/TC) mode exploring the DMFc$^+$ cation transfer across the liquid/liquid interface. The potential of the tip allowed for the reduction of the redox-active cations ejected from the NPOE phase due to the electrooxidation of DMFc. Two
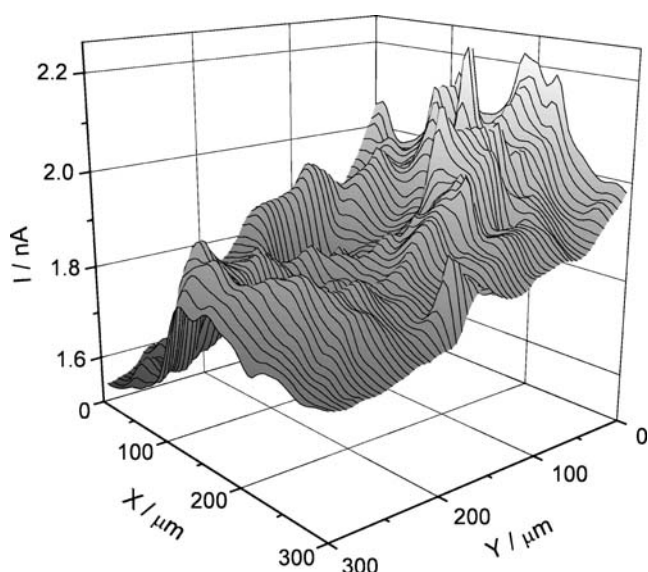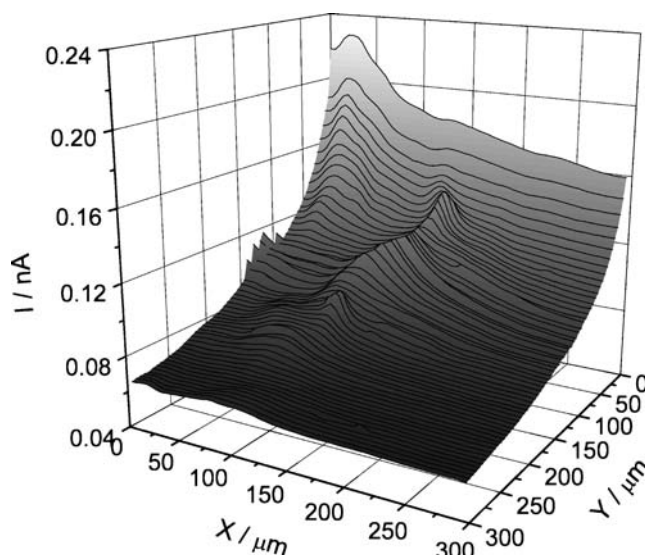
important features of the SECM image are clearly visible (Fig. 9): (1) substantial decrease of the current during scanning and (2) areas of enhancement or decrease of current flow. The first effect is probably connected with the formation of DMFc deposit on the tip (see above) blocking the electrode surface. In addition, the consumption of DMFc from the organic phase and the decrease of the flux of DMFc$^+$ from CCE can also cause the decrease of the current during scanning. The second effect may result from the distribution of the three-phase junction, electrode/ NPOE/aqueous electrolyte, where reaction 1 is the most likely to occur due to a heterogeneous structure of CCE. This reaction is clearly followed by the outflow of electro-generated DMFc$^+$ cations transferred from the organic to the aqueous phase.

Fig. 8 SECM image of the CCE modified with NPOE. Other conditions as in Fig. 7
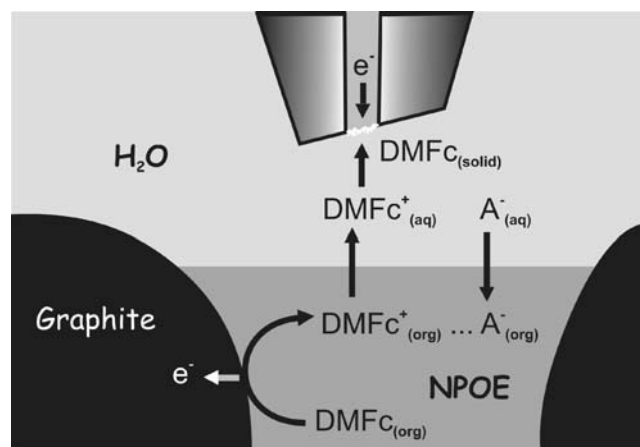
Scheme 2 A schematic presentation of the studied process

Conclusions

Using a SECM apparatus, the transfer of the hydrophobic $DMFc^+$ cation across the NPOE/aqueous solution interface formed at the CCE surface was detected. The $DMFc^+$ cations transferred into the aqueous phase were detected on the SECM tip near the CCE surface. The overall electrode process including the reaction at the tip and the substrate is summarized in Scheme 2. The $DMFc^+$ cation transfer across the liquid/liquid interface occurs despite the hydrophobic nature of the ferrocene cation bearing ten methyl groups. This process is more pronounced in the presence of hydrophilic Cl^- anions in the aqueous phase in comparison to the ClO_4^- aqueous solution. This is caused by the lower ability of the former anion to enter the hydrophobic NPOE phase.

The reflection of a heterogeneous structure of CCE composed of aggregates of electronically conductive graphite particles and an isolating hydrophobic silicate is observed on the SECM image of CCE and the same electrode modified by the redox probe solution in the organic phase. This clearly indicates the presence and role of the three-phase junction, graphite/organic solvent/aqueous phase, in the electrode reaction consisting of a heterogeneous electron transfer reaction in the organic phase followed by the ion transfer across the liquid/liquid interface.

References

1. Volkov AG (ed) (2001) Liquid interfaces in chemical, biological and pharmaceutical applications. Marcel Dekker, New York
2. Marken F, Webster RD, Bull SD, Davies SG (1997) J Electroanal Chem 437:209
3. Scholz F, Komorsky-Lovric S, Lovric M (2000) Electrochem Commun 2:112
4. Tasakorn P, Chen J, Aoki K (2002) J Electroanal Chem 533:119
5. Shul G, Opallo M (2005) Electrochem Commun 7:194
6. Banks CE, Davies TJ, Evans RG, Hignett G, Wain AJ, Lawrence NS, Wadhawan JD, Marken F, Compton RG (2003) Phys Chem Chem Phys 5:4053
7. Bak E, Donten M, Stojek Z (2005) Electrochem Commun 7:483
8. Scholz F, Schroder U, Gulaboski R (2005) Electrochemistry of immobilized particles and droplets. Springer, Berlin, p 209
9. Tsionsky M, Gun G, Glezer V, Lev O (1994) Anal Chem 66:1747
10. Rabinovich L, Lev O (2001) Electroanalysis 13:265
11. Opallo M, Saczek-Maj M (2001) Electrochem Commun 3:306
12. Opallo M, Saczek-Maj M (2002) Chem Commun 448
13. Shul G, Opallo M, Marken F (2005) Electrochim Acta 50:2315
14. Saczek-Maj M, Opallo M (2003) Electroanalysis 15:566
15. Opallo M, Saczek-Maj M, Shul G, Hayman CM, Bulman Page PC, Marken F (2005) Electrochimica Acta 50:1711
16. Scholz F, Gulaboski R (2005) Chem Phys Chem 6:16
17. Gulaboski R, Galland A, Bouchard G, Caban K, Kretschmer A, Carrupt PA, Stojek Z, Girault HH, Scholz F (2004) J Phys Chem B 108:4565
18. Bak E, Donten M, Stojek Z (2007) J Electroanal Chem 600:45
19. Schuhmann W, Wohlschlager H, Lammert R, Schmidt H-L, Loffler U, Wiemhofer H, Gopel DW (1990) Sens Actuators B 1:571
20. Bard AJ, Mirkin MV (2001) Scanning electrochemical microscopy. Marcel Dekker, New York
21. Mirkin MV, Horrocks BR (2000) Anal Chim Acta 406:119
22. Barker AL, Gonsalves M, Macpherson JV, Slevin CJ, Unwin PR (1999) Anal Chim Acta 385:223
23. Sun P, Laforge FO, Mirkin MV (2007) Phys Chem Chem Phys 9:802
24. Shao Y, Mirkin MV (1998) J Phys Chem B 102:9915
25. Cai C, Tong Y, Mirkin MV (2004) J Phys Chem B 108:17872
26. Donten M, Stojek Z, Scholz F (2002) Electrochem Commun 4:324
27. Goldfarb DL, Corti HR (2001) J Electroanal Chem 509:155
28. Mandal AB (1993) Langmuir 9:1932
29. Dietz S, Bell WL, Cook RL (1997) J Organomet Chem 545–546:67
30. Ryabov AD, Ryabova ES, Reshetova MD (2001) J Organomet Chem 637–639:469
31. Wilke S, Zerihun T (2001) J Electroanal Chem 515:52
32. Bond AM, Marken F (1994) J Electroanal Chem 372:125
33. Oskam G, Searson PC (1998) J Phys Chem B 102:2464